

APPS/PSNZ Meeting - Sydney 2003

Poster Session 2

Tuesday 30th September 2003

Effect of oscillating airway smooth muscle length on bronchoconstriction – the role of the airway wall

P.B. Noble, P.K. McFawn and H.W. Mitchell, School of Biomedical and Chemical Sciences, University of Western Australia, Crawley, WA 6009, Australia.

A period of deep inspiration in man is known to modulate subsequent bronchoconstriction (Crimi *et al.*, 2002; Kapsali *et al.*, 2000), an effect which may be elicited through direct stretch of airway smooth muscle (ASM). We investigated the response of porcine ASM to a period of length oscillation in three different preparations: whole bronchial segments; bronchial segments which had cartilage removed; and isolated ASM strips. ASM response to electrical field stimulation (EFS) was assessed before and at different time points after ASM length oscillation. In bronchial segments oscillation of ASM length was achieved by cycling intraluminal pressure from 5 to 25cmH₂O, while in isolated ASM length changes were directly imposed. In each of the three preparations the amplitude of length oscillation was 20-25% of resting ASM length cycled at 0.5Hz for a period of 10 minutes. ASM length and cartilage area were morphometrically determined in airways fixed at 5 and 25cmH₂O. In whole bronchial segments response to EFS was increased immediately after ASM length oscillation ($P<0.05$). In contrast to whole airways, 5 out of 7 cartilage-denuded airways had reduced response to EFS following length oscillation ($P<0.05$). ASM lengths were not significantly different between control and cartilage-denuded airways at either 5 or 25cmH₂O. Post oscillation response to EFS was positively correlated to airway wall cartilage ($P<0.05$). In isolated ASM, response to EFS was reduced immediately after length oscillation ($P<0.01$). In each preparation the effect of length oscillation was absent 10 minutes after oscillation had concluded. Our results show that the response of ASM to length oscillation is strongly influenced by the airway wall. Length oscillation enhanced ASM contraction *in situ*, but depressed contraction in isolated ASM. Following cartilage removal, the response of ASM to length oscillation mimicked the depression in contraction observed in isolated ASM, suggesting airway wall structure plays a substantial role in the effect observed with oscillation.

Crimi, E., Pellegrino, R., Milanese, M. & Brusasco, V. (2002) *Journal of Applied Physiology*, 93, 1384-1390.

Kapsali, T., Permutt, S., Laube, B., Scichilone, N. & Togias, A. (2000) *Journal of Applied Physiology*, 89, 711-720.

Bronchial response to protease-activated receptor stimulation of airway luminal and adventitial surfaces

H.W. Mitchell, H.L. Goh, N. Asokanathan, R.S. Lan, G.A. Stewart and A. Sharma, School of Biomedical and Chemical Sciences, University of Western Australia, Nedlands, WA, Australia.

A recently characterised family of G protein coupled receptors, protease-activated receptors (PARs), modulate inflammatory and regulatory signals in the airway. There are currently four PARs (PAR1, PAR2, PAR3 and PAR4) that have been cloned and characterised. Trypsin is an endogenous activator of PAR2 and PAR4. Activating these PARs has been shown to release PGE₂ from airway epithelial cells and modulate smooth muscle tone in isolated airway preparations (Cocks *et al.*, 1999; Lan *et al.*, 2001). It is uncertain how these different actions of PARs expressed on the various cell types in the airway may modulate airway function where luminal and adventitial surfaces can be separately accessed by PAR activators. The present study investigates the actions of trypsin (300 µg/ml) and PAR agonist peptides (100-400 nM) on isolated whole airways in which the epithelial and adventitial surfaces can be separately exposed to PAR agonists. Bronchial airways were dissected from the lungs of pigs. Side branches were ligated and segments were placed in a bath at 37°C so that luminal and adventitial surfaces were bathed in Krebs solution. A pressure transducer measured airway luminal pressure, from which airway responses were assessed. Luminal Krebs solution was assayed for PGE₂ by ELISA. Trypsin added to the adventitia produced a short latency (<5 min) inhibition of carbachol-induced tone. However, trypsin added to the airway lumen produced a delayed (>45 min) suppression of acetylcholine dose-contraction curve. Moreover, both trypsin and the PAR2 agonist increased PGE₂ production. Indomethacin pre-treatment blocked production of PGE₂, but had no effect on trypsin-induced relaxation by either route. The PAR1, 2 and 3 agonists had no effect on airway tone, but the PAR4 agonist produced short latency relaxation that was blocked by indomethacin. The study confirms that trypsin relaxes airways and releases PGE₂. Moreover, the effects of trypsin are highly dependent on its route of delivery, suggesting the contribution of different cell types by each route of exposure. However, the results observed with trypsin and the PAR2 agonist appear to dissociate the possible link between PGE₂ release by PAR activation and subsequent airway relaxation in this whole airway preparation. These findings suggest that the functional responses to trypsin are likely to be mediated by a receptor other than the established PAR1, PAR2, PAR3 or PAR4.

Cocks, T.M., Fong, B., Chow, J.M., Anderson, G.P., Frauman, A.G., Goldie, R.G., Henry, P.J., Carr, M.J., Hamilton, J.R. & Moffatt, J.D. (1999) *Nature*, 398, 156-160.

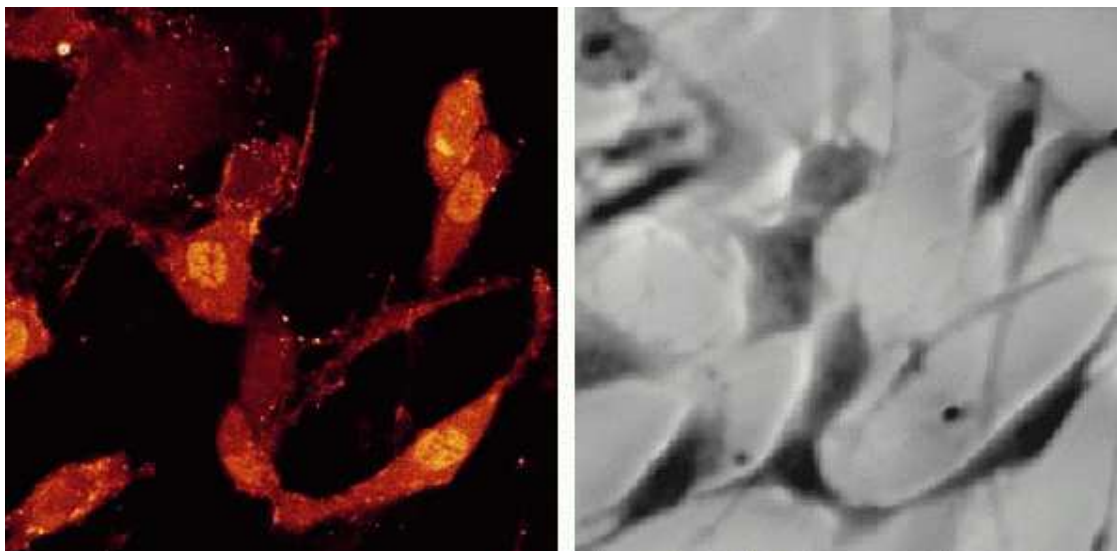
Lan, R.S., Knight, D.A., Stewart, G.A. & Henry, P.J. (2001) *British Journal of Pharmacology*, 132, 93-100.

Measurement of culture confluency and volume of human airway smooth muscle cells using quantitative phase microscopy

C.L. Curl¹, C.J. Bellair², T. Harris³, B.E. Allman⁴, A. Roberts², K.A. Nugent², P.J. Harris¹, A.G. Stewart³ and L.M.D. Delbridge¹, ¹Department of Physiology, ²Department of Physics, and ³Department of Pharmacology, University of Melbourne, Parkville, Victoria 3010 and ⁴IATIA Ltd., Rutland Rd, Box Hill, Victoria 3128, Australia.

Quantitative Phase Microscopy (QPM) is a recently developed computational approach that provides quantitative phase measurements of images captured using a bright-field microscope. Phase measurement is particularly useful in the evaluation of translucent objects, such as unstained viable cell specimens. QPM works via an algorithm which is applied to a standard bright-field and equidistant positive and negative de-focus images. From these images a phase map is generated which contains information about cell thickness and refractive index and can allow quantitation of cellular structure. QPM was used in conjunction with laser scanning confocal microscopy (LSCM) to measure volume and area in cultured human airway smooth muscle (HASM) cells.

HASM cells were obtained by collagenase and elastase digestion of smooth muscle from lung transplant resection patients. The resulting cell suspension was washed in phosphate buffered saline and seeded onto glass coverslips which were placed in the base of a plastic culture dish at 37°C in Dulbecco's Modified Eagles Media. The cells were imaged using both LSCM (optical slicing) and QPM techniques. For LSCM visualisation, cells were fluorescently labelled (fluo-3/AM, Molecular Probes, Eugene, OR, USA) and a series of images in the vertical (z) axis were recorded at intervals of 1µm using a Leica TCS 4D (x63, PL APO 1.40 NA oil immersion objective). From these images a calculation of cell depth was performed. Phase images of the same field of cells were then obtained using an inverted Zeiss Axiovert 100M microscope (×10, LD-Achroplan 0.3 NA objective) and a Coolsnap fx CCD camera (Photometrics, USA). Phase calculations were performed using QPM software (v2.0 IATIA Ltd, Australia).



On the basis of the cell depth determined by LSCM (left panel of Figure) and the phase measurements calculated by QPM (right panel of Figure) a mean refractive index (RI) for HASM was determined to be 1.4275 ± 0.009 . This RI was then used computationally by the QPM algorithm to determine cellular volume. The relationship between cell confluency and volume in HASM cultures passaged for variable periods was evaluated. The confluency of cells (% field area), calculated over a 92 hour growth period from phase maps and cell volume (μm^3) were highly correlated (i.e. r^2 values of 0.986 and 0.996 obtained for two different cell culture lines). Thus, in these HASM cells under the conditions specified, there is a well defined relationship between extent of confluence and total cell volume in culture. QPM provides a convenient procedure for estimating cell volume, where prior determination of RI is required. We have demonstrated that this may be achieved by parallel specimen imaging using both LSCM and QPM.

Increases in renal angiotensinogen mRNA levels following a mixed amino acid infusion in late gestation fetal sheep

A.C. Boyce, K.J. Gibson, J. Wu and E.R. Lumbers, Dept of Physiology & Pharmacology, School of Medical Sciences, University of New South Wales, Sydney 2052, Australia.

We have previously reported that prolonged infusions of amino acids to fetal sheep in late gestation stimulated renal growth, had profound, sustained effects on fetal renal function (including increases in glomerular filtration rate, renal blood flow, a diuresis, natriuresis and increased osmolar excretion), and induced changes indicative of extracellular volume expansion (Marsh *et al.*, 1999, Marsh *et al.*, 2002). This study aimed to determine whether the fetal renin-angiotensin system was also affected when plasma amino acid levels were increased long term.

Fetal sheep were chronically catheterised under general anaesthesia induced with 1 g sodium thiopentone i.v. and maintained with 2-3% halothane in oxygen. At least 5 days after surgery, 5 fetuses aged 122 ± 1 days gestation (term ~ 150 days) were infused i.v. for 7 days with a mixture of alanine, glycine, proline and serine (1:1:0.6:0.6) at $0.22 \text{ mmol min}^{-1}$ and 5 mL h^{-1} . Six control fetuses were infused with 0.15 M saline. Plasma and renal renin levels were measured as the rate of formation of angiotensin I (Ang I) when plasma or homogenates of renal cortex were incubated at 37°C and pH 7.4 with an excess of angiotensinogen (nephrectomised sheep plasma). Levels of mRNA for renin, angiotensinogen and the angiotensin receptor subtypes I and II (AT_1R and AT_2R) were measured in renal cortical homogenates by real time PCR, and expressed relative to a calibrator sample.

After 7 days of amino acid infusion, plasma concentrations of the infused amino acids had increased by between 8- and 36-fold ($P < 0.05$), and kidney weights were $\sim 28\%$ greater than those of control fetuses ($P < 0.05$). Circulating renin levels fell during the first 4 h, from 9.3 ± 2.1 (mean \pm SE) $\text{ng Ang I mL}^{-1} \text{ h}^{-1}$ in control to 4.7 ± 1.5 ($P < 0.05$), and remained low throughout the infusion (Day 4: 4.2 ± 2.5 , n.s.; Day 7: $2.2 \pm 1.1 \text{ ng mL}^{-1} \text{ h}^{-1}$, $P < 0.05$). Plasma renin levels did not change during saline infusion (baseline: $5.9 \pm 1.6 \text{ ng Ang I mL}^{-1} \text{ h}^{-1}$). Renal renin levels tended to be lower following amino acid infusion compared to control fetuses (1.1 ± 0.4 vs $2.1 \pm 0.4 \mu\text{g Ang I mg protein}^{-1} \text{ h}^{-1}$, n.s.). Renal renin mRNA levels were also lower (Amino acids: 3.6 ± 2.2 ; Saline: 10.5 ± 2.7 , $P = 0.075$). There was marked increase in renal angiotensinogen mRNA levels (3.6 ± 0.5 vs 1.4 ± 0.2 , $P < 0.005$). Renal AT_1R and AT_2R mRNA levels were not different between groups.

Prolonged increases in fetal plasma amino acid levels were therefore associated with a suppression of circulating renin levels, and tended to suppress the gene expression and levels of renin in the developing kidney. These changes were probably secondary to volume expansion. However, the stimulation of renal angiotensinogen gene expression by amino acids suggests that the renal renin-angiotensin system may have played a role in the stimulation of renal function and growth that occurred with amino acid infusion.

Marsh, A.C., Gibson, K.J. & Lumbers, E.R. (1999) *Proceedings of the Australian Society for Medical Research*, Oral 8-1.

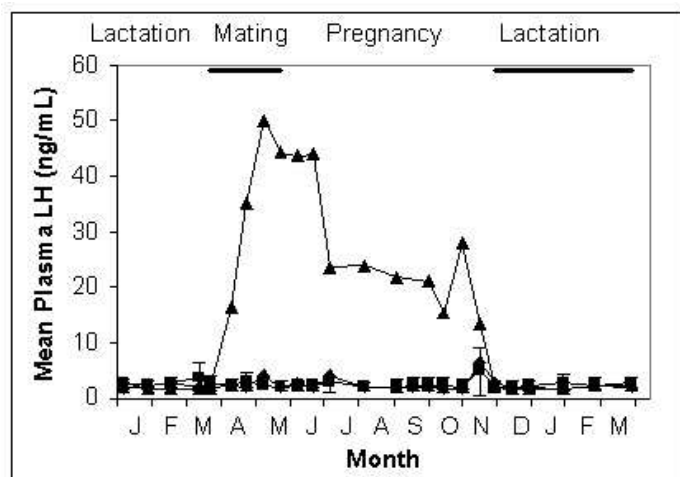
Marsh, A.C., Gibson, K.J. & Lumbers, E.R. (2002) *Journal of Physiology* **540**, 717.

Central program and ovarian feedback both influence LH secretion in flying-foxes

G.M. O'Brien and K.-A. Gray, School of Biological, Biomedical and Molecular Sciences, University of New England, NSW 2351, Australia.

Very large changes in plasma progesterone and oestradiol are observed during late pregnancy, in Australia's greyheaded flying-fox, *Pteropus poliocephalus*, but changes associated with ovulation are enigmatic. Attempts to identify the time of ovulation by monitoring peripheral hormones have been so unsuccessful that a question has arisen as to the nature of feedback between the ovary and the hypothalamus-pituitary axis in these animals. *P. poliocephalus* mate during April-May and deliver a single young in October-November. In captivity they can live for 20-30 years but wild populations are listed as 'threatened' under the Environment Protection and Biodiversity Conservation Act. Understanding their reproductive physiology is essential for recovery of the species. Important stages of reproduction, including ovulation, are regulated by luteinising hormone (LH) but plasma LH has not previously been measured in the Order Megachiroptera. Recent development of an assay for flying-fox LH (O'Brien *et al.*, in press) has made it possible to test for the effects of reproductive stage (copulation, pregnancy etc.) and ovarian feedback on mean plasma LH levels in female flying-foxes through an entire annual cycle of reproduction.

Methods. Blood samples were collected by venipuncture (O'Brien *et al.*, 1996), at intervals of 1 to 4 weeks. LH was measured by ^{125}I -RIA using monoclonal antibody 518B7, and ovine LH (oLH-G3-330-Br) as radioligand and standard (O'Brien *et al.*, in press). Animals were housed in a single-sex group (segregated \blacklozenge $n=4$) or in a large mixed-sex group (breeding \blacksquare sub-set $n=5$); each group had a long-term ovariectomised female with them (ovariectomised \blacktriangle data are average of 2).



Results shown in the Figure clearly demonstrate three phases of LH secretion during the year in the absence of ovarian steroid feedback (ovariectomised \blacktriangle): very high levels Apr-May; elevated levels Jun-Oct; baseline levels Nov-Mar. Mean plasma LH remained at baseline all year in intact animals (\blacklozenge , \blacksquare : Figure shows means and SD).

Discussion. The pituitary appears to be programmed to stimulate the ovaries from mid-autumn (April) until mid-spring (October) (see the Figure). Pituitary content of LH is high during April-May (O'Brien *et al.*, in press). However strong negative feedback from the ovaries reduced the frequency and/or

amplitude of LH pulses so dramatically that no elevation of mean plasma levels was observed in intact animals. There was no indication of the timing of ovulation. During pregnancy, placental steroids probably also contributed to the feedback.

The phase of the central program revealed during June-October probably provides a safety net in the event of early pregnancy loss and if so, would explain the occasional late births that are recorded. It may also provide the physiological substrate for the observed geographic variation in breeding times of a congeneric species, *P. alecto* (Vardon & Tidemann 1998).

The November-March phase reveals a centrally programmed anoestrus not previously known. This may explain why variations in the timecourse of lactation do not influence timing of the subsequent pregnancy (unpub. obs.).

O'Brien, G.M., Curlewis, J.D. & Martin, L. (1996) *General & Comparative Endocrinology* 104, 304-311.

O'Brien, G.M., McFarlane, J.R. & Kearney, P.J. (in press) *Reproduction, Fertility and Development*.

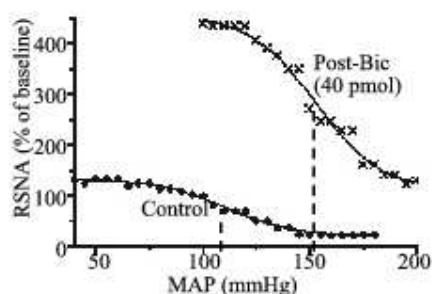
Vardon, M.J. & Tidemann, C.R.. (1998) *Australian Journal of Zoology*, 46, 329-344.

The dorsomedial hypothalamic nucleus modulates the baroreceptor reflex

L.M. McDowall, S. Killinger and R.A.L. Dampney, Department of Physiology F13, University of Sydney, NSW 2006 Australia.

The dorsomedial hypothalamic nucleus (DMH) plays a critical role in mediating the increase in arterial pressure and heart rate evoked by an acute stress (Stotz-Potter, *et al.*, 1996). The cardiovascular changes evoked by acute stress are also associated with modulation of the baroreceptor reflex (Spyer, 1994). The aim of this study was to determine if the DMH is capable of modifying the baroreceptor reflex control of heart rate and sympathetic vasomotor activity.

Experiments were performed on rats anaesthetised with urethane (1.35g/kg i.p.). Arterial pressure, heart rate (HR) and renal sympathetic nerve activity (RSNA) were measured. The baroreceptor reflex function was determined by measuring the changes evoked in HR and RSNA by alterations in mean arterial pressure (MAP) over a wide range (50-200 mmHg), induced by intravenous infusions of a vasodilator (sodium nitroprusside) or vasoconstrictor (phenylephrine). In each experiment, baroreceptor reflex function curves were determined before and after microinjection of the GABA receptor antagonist bicuculline (4 or 40 pmol) or the vehicle solution of artificial cerebrospinal fluid (ACSF) into the DMH. A logistic function curve of best fit was calculated in each case.



As illustrated in the Figure, disinhibition of DMH neurons by bicuculline microinjection resulted in a shift in the baroreceptor reflex function curve. The baroreceptor reflex operating point (OP, dashed line) for the baroreflex control of both HR and RSNA was significantly increased (* $P < 0.05$) in a dose-dependent fashion by bicuculline microinjection, but not ACSF microinjection into the DMH (see the Table below). There was no reduction, however, in the gain of the renal sympathetic or cardiac component of the baroreceptor reflex.

		Δ OP (mm Hg)	
Bic (pmol)	n	HR	RSNA
0 (ACSF)	6	0 \pm 2.6	3 \pm 1.9
4	6	15 \pm 4.1*	9 \pm 2.4*
40	6	26 \pm 4.1*	18 \pm 5.7*

We conclude that activation of the DMH alters the operating point of the baroreceptor reflex, but that the reflex remains operational over a wide range of arterial pressures.

Spyer, K.M. (1994) *Journal of Physiology*, 474, 1-19.

Stotz-Potter, E.H., Willis, L.R. & DiMicco, J.A. (1996) *Journal of Neuroscience*, 16, 1173-1179.

Renal sympathoexcitatory response evoked from the dorsomedial hypothalamic nucleus is mediated by presympathetic vasomotor neurons in the rostral ventrolateral medulla

J. Horiuchi¹, S. Killinger¹, R.M. McAllen², A.M. Allen² and R.A.L. Dampney¹, ¹Department of Physiology, The University of Sydney, NSW 2006, Australia and ²Neurobiology Group, The Howard Florey Institute, The University of Melbourne, VIC 3010, Australia.

The dorsomedial hypothalamic nucleus (DMH) plays a critical role in mediating the cardiovascular response to an acute stress (Stotz-Potter, *et al.*, 1996). Activation of neurons in the DMH causes an increase in arterial pressure, heart rate and renal sympathetic nerve activity (Fontes *et al.*, 2001). We have previously shown that the sympathoexcitatory vasomotor, but not cardiac, component of the DMH-evoked response is dependent upon a synapse in the rostral ventrolateral medulla (Fontes *et al.*, 2001). On the other hand, Samuels *et al.* (2002) showed that the cardiac component of the response is mediated by neurons in the midline raphe pallidus (RP) in the medulla, but did not examine the sympathoexcitatory vasomotor component. The aims of this study were (1) to determine if inhibition of RP neurons affects the sympathoexcitatory component of the DMH-evoked response, and (2) to determine the extent to which, at the single neuron level, RVLM presympathetic neurons are influenced by inputs from the DMH.

Experiments were performed on rats anaesthetised with urethane (1.4 g/kg i.p). Mean arterial pressure (MAP), heart rate (HR) and either renal sympathetic nerve activity (RSNA) or the extracellular activity of barosensitive and spinally-projecting RVLM neuron were recorded. Unilateral microinjections of the GABA receptor antagonist bicuculline (0.1-40pmol in 20nl) into the DMH resulted in dose-dependent increases in MAP, HR and rSNA. Inhibition of the RP by injections of muscimol (80pmol in 100nl) did not alter the increase in rSNA evoked by bicuculline (40pmol) in the DMH, whereas increases in MAP and HR were significantly attenuated, as Samuels *et al.* (2002) previously reported. In addition, the extracellular activity of 5 out of 6 barosensitive and spinally-projecting neurons in the RVLM were strongly excited (increase in firing rate of $417 \pm 125\%$) by unilateral injection of bicuculline (40pmol) into the DMH. The results demonstrate that the cardiac and sympathoexcitatory vasomotor components of the cardiovascular response elicited by disinhibition of the DMH are mediated via at least two different descending pathways in the medulla.

Fontes, M.A., Tagawa, T., Polson, J.W., Cavanagh, S.J. & Dampney, R.A.L. (2001) *American Journal of Physiology*, 280, H2891-H2901.

Samuels, B.C., Zaretsky, D.V. & DiMicco, J.A. (2002) *Journal of Physiology*, 538, 941-946.

Stotz-Potter, E.H., Willis, L.R. & DiMicco, J.A. (1996) *Journal of Neuroscience*, 16, 1173-1179.

Blockade of angiotensin type 1 (AT1) receptors in the rostral ventrolateral medulla increases renal sympathetic activity and arterial pressure under hypoxic conditions

J. Sheriff, M.A.P. Fontes, S. Killinger and R.A.L. Dampney, Department of Physiology F13, University of Sydney, NSW 2006, Australia.

Administration of exogenous angiotensin II (AngII) into the rostral ventrolateral medulla (RVLM) increases sympathetic activity and blood pressure, indicating that it has an excitatory effect on presympathetic neurons in this region. Blockade of angiotensin type 1 (AT1) receptors in the RVLM under normal conditions results in little change in sympathetic activity, suggesting that under these conditions endogenous AngII has little tonic effect in the RVLM. Recently, however, it has been suggested that endogenous Ang II has a tonic action on both excitatory and inhibitory mechanisms in the RVLM, so that the ultimate effect on sympathetic activity depends upon the balance between the excitatory and inhibitory effects of endogenous AngII on presympathetic neurons (Hu *et al.*, 2002). If that is the case, then this balance could be altered under conditions in which the level of activity of excitatory or inhibitory synaptic inputs to RVLM neurons is altered. In this study we have tested this hypothesis by determining the effects of blockade of AT1 receptors in the RVLM under hypoxic conditions, which is known to enhance the excitatory glutamatergic inputs to RVLM presympathetic neurons. Rats were anaesthetised with urethane (I.P. 1.35g/kg) and arterial pressure, heart rate and renal sympathetic nerve activity were recorded. Unilateral microinjections of an AT1 receptor antagonist, candesartan (100pmol), into the RVLM during moderate hypoxia (PO₂ 10%) resulted in an increase in arterial pressure and renal sympathetic nerve activity, whereas microinjections of the vehicle solution had little effect. The results indicate that, under hypoxic conditions, endogenous AngII has a net tonic sympathoinhibitory effect. Taken together with other recent findings, the results are consistent with the hypothesis that AT1 receptors can mediate both tonic excitatory and inhibitory effects on RVLM sympathoexcitatory neurons, and the balance of these effects is altered under different physiological conditions.

Hu, L., Zhu, D., Yu, Z., Wang, J.Q., Sun, Z. & Yao, T. (2002) *Journal of Applied Physiology*, 92, 2153-2161.

Angiotensin II microinjections in the nucleus tractus solitarius has an inhibitory effect on the cardiac but not the non-cardiac sympathetic component of the baroreceptor reflex

P. Tan and R.A.L. Dampney, Department of Physiology F13, University of Sydney, NSW 2006, Australia.

The nucleus tractus solitarius (NTS) is a major nucleus located in the dorsal medulla and is critical in the mediation of the baroreceptor reflex. It is also a site which contains a high density of high affinity binding sites for angiotensin II (AngII). Previous studies have shown that microinjections of AngII cause significant inhibition of the cardiac component of the baroreceptor reflex. However there is very little information on its effects on the non-cardiac sympathetic component, which is of critical importance in the regulation of blood pressure. Experiments were carried out in adult male Sprague-Dawley rats that were initially anaesthetised with pentobarbital sodium (60mg/kg, I.P.) and maintained by I.V. infusion of pentobarbital sodium (6mg/ml at 1-1.3ml/hr). The arterial pressure, heart rate (HR) and renal sympathetic nerve activity (RSN) were measured. The baroreceptors were stimulated by increases in mean arterial pressure (MAP) of 40-50 mmHg induced by a single bolus injection of phenylephrine, and the reflex decrease in HR and RSN measured.

Following bilateral microinjections of 40pmol AngII (50nl) into the NTS, the gain of the cardiac component of the reflex (measured as $\Delta\text{HR}/\Delta\text{MAP}$) was greatly reduced by $70 \pm 8.7\%$ compared with that before Ang II microinjections. In contrast, bilateral microinjections of AngII into the NTS had no significant effect (change of $1.4 \pm 5.5\%$) on the gain of the renal sympathetic component of the reflex (measured as $\Delta\text{RSNA}/\Delta\text{MAP}$). In control experiments, bilateral microinjections of the vehicle solution into the NTS had no effect on the gain of either the cardiac or renal sympathetic component of the reflex.

We conclude from these experiments that the inhibitory influence of AngII microinjections may be restricted to the cardiac component of the baroreflex. It is possible that in conditions where endogenous AngII activity is increased (e.g. hypertension or heart failure) the cardiac reflex response to changes in blood pressure may be inhibited, whereas the baroreceptor mediated vasomotor response is largely unaffected.

Angiotensin II via AT₁ receptors may mediate apoptosis in the cardiac conduction system of rats

U. Vongvatcharanon¹, S. Vongvatcharanon², N. Radenahmad¹, P. Kirirat¹, P. Intasaro¹, P. Sobhon³ and T. Parker⁴, ¹Department of Anatomy, Faculty of Science, Prince of Songkla University, Hat-Yai 90112, Thailand, ²Department of Oral Surgery, Faculty of Dentistry, Prince of Songkla University, Hat-Yai 90112, Thailand, ³Department of Anatomy, Faculty of Science, Mahidol University, Bangkok 10400, Thailand and ⁴School of Biomedical Science, Nottingham University, Nottingham NG7 2UH, UK.

Apoptosis has been suggested as a possible cause of gradual development of complete heart block and fatal arrhythmias associated with absence of the AV node, sinus, and internodal pathways (James *et al*, 1996). Studies about apoptosis in the heart by means of cardiomyocyte cell culture have demonstrated that angiotensin II (Ang II) mediates cardiomyocyte apoptosis via angiotensin II type I receptors (AT₁) (Cigola *et al*, 1997). The transgenic *m(Ren-2)27* (TG) rat carries the additional *Ren-2* gene, the expression of which results in an increase of heart Ang II (Campbell *et al*, 1995), thus potentially affecting the cell growth/death equilibrium. This study addresses the question of role of Ang II/AT₁ receptors mediated apoptosis in the sinoatrial (SA) and atrioventricular nodes (AV).

Six, male 2 week TG and Hannover Sprague Dawley (SD) rats were anaesthetised by pentobarbitone sodium i.p. injection (100 mg/kg). The hearts were removed and fixed in 10% formaldehyde. Following dehydration and embedding in paraffin, 5 µm serial sections were cut then stained with Masson Trichrome to localize SA and AV nodes. The sections containing SA or AV node were processed for either: (a) calculation of apoptotic nuclei following terminal deoxynucleotidyl transferase nick end labelling of 3'-OH ends using Fluorescein-FragEL™; or (b) immunohistochemical labelling with antibodies to the AT₁ receptors prior to confocal scanning laser microscopical analysis. Quantification of AT₁ receptors was performed by using Microimage analysis software (Olympus).

Group	Apoptotic cells/mm ²		AT ₁ receptors (×10 ³)/mm ²	
	SA	AV	SA	AV
SD	0.040±0.07	0.164±0.12	1.14±0.17	7.63±1.91
TG	0.140±0.37*	0.433±0.11*	1.67±0.26*	12.50±3.97*

Data expressed as mean ± SD (n=6)

* = significant compared with control (P<0.05) (Independent-Sample T-test)

The table shows that the number of apoptotic cell in both the SA and AV node is significantly greater in the TG compared with the SD (p<0.05). Quantification of AT₁ receptors within SA and AV node shows that there were significantly more AT₁ receptors in the TG compared with the SD (p<0.05). These data suggest that an elevated level of apoptosis in the TG rat heart compared with the controls could be accounted for by *Ren-2* derived Ang II active via AT₁ receptors.

Campbell, D.J., Rong, P., Kladis, A., Rees, B., Ganten, D. and Skinner, S.L. (1995) Angiotensin and Bradykinin peptides in the TGR (*mRen-2*)27 rat. *Hypertension*, 25, 1014-1020.

Cigola, E., Kajstura, L.B., Meggs, L.G. and Anversa, P. (1997) Angiotensin II activates programmed myocyte cell death *in vitro*. *Experimental Cell Research*, 231, 363-371.

James, T.N., Martin, E., Willis, P.W. and Lohr, T.O. (1996) Apoptosis as a possible cause of gradual development of complete heart block and fatal arrhythmias associated with absence of the AV node, sinus, and internodal pathways. *Circulation*, 93, 1424-1432.

Effect of sinoaortic denervation on baroreflex sensitivity assessed with complex demodulation in the anaesthetised rat

Y.C. Tzeng, P.D. Larsen and D.C. Galletly, Department of Surgery and Anaesthesia, Wellington School of Medicine, PO Box 7343, Wellington, New Zealand.

The relevance of baroreflex dysfunction in the clinical setting has stimulated a rapidly expanding area of research into the assessment of baroreflex sensitivity (BRS). Recent efforts have concentrated on developing non-invasive techniques that allow BRS to be determined from spontaneous heart rate and blood pressure recordings, such as the sequence method and the α -index. However, these techniques are limited as they provide average estimates over the entire period of recorded data. More recently, Kim & Euler (1997) introduced an alternative method of estimating BRS from spontaneous heart rate and blood pressure fluctuations based on complex demodulation (CMD) that is capable of assessing the dynamic changes in cardiovascular variability and baroreflex sensitivity as a function of time (Hayano *et al.* 1993). Using an anaesthetised rat model, the current study was conducted to validate the use of CMD analysis in sinoaortic denervated rats, and compare its performance to the Oxford method, sequence technique and α -index.

In 12 anaesthetised rats breathing isoflurane (1.5-2%) through a tracheal cannula, we recorded the ECG and continuous arterial blood pressure before and after sinoaortic denervation (SAD). Arterial baroreflex testing using the Oxford method was performed before and after SAD using similar doses of phenylephrine ($1.5 \mu\text{g kg}^{-1}$) and sodium nitroprusside ($2.5 \mu\text{g kg}^{-1}$) in 0.3 ml over 15 s administered intravenously. From spontaneous HR and SBP recordings we determined non-invasive BRS using CMD, sequence technique and the α -index.

Consistent with Kim & Euler's study, we found that BRS values obtained with CMD was strongly correlated to values derived from phenylephrine ($R=0.83$, $P<0.01$), nitroprusside ($R=0.77$, $P<0.01$), sequence technique ($R=0.85$, $P<0.01$) and α -index ($R=0.78$, $P<0.01$). The absolute values of BRS estimates obtained with CMD was similar to sequence technique and α -index, but were significantly greater than values obtained with the Oxford method. Following SAD, Oxford measures of BRS decreased to almost 0, while CMD and sequence techniques showed 50% reductions. The α -index method showed no significant decrease following SAD.

We conclude that the CMD approach to measuring BRS is at least as accurate as the sequence technique and is superior to the α -index. All three non-invasive measures differ markedly from the Oxford measure. The fine temporal resolution offered by CMD, and the high correlation with the Oxford method mean that this technique would be very useful as an index of BRS under conditions in which BRS is changing rapidly, and invasive measures are not possible.

Kim S.Y. & Euler D.E. (1997) *Hypertension*, 29, 1119-1125.

Hayano, J., Taylor, J.A., Yamada, A., Mukai, S., Hori, R., Asakawa, T., Yokoyama K., Watanabe. Y., Takata. K. & Fujinami. T. (1993) *American Journal of Physiology*, 264, H1229-H1238.

Change in baroreflex sensitivity during induction of anaesthesia with propofol

P.D. Larsen, Y.C. Tzeng and D.C. Galletly, Department of Surgery & Anesthesia, Wellington School of Medicine, PO Box 7343, Wellington, New Zealand.

A number of studies have demonstrated that general anaesthesia with propofol results in a decrease in baroreflex sensitivity (BRS), and suggested that this is due to inhibition of sympathetic nervous activity (Ebert *et al.*, 1992, Sellgren *et al.*, 1994). These studies have compared pre-anaesthetic measures with measurements taken following induction, once a steady state of anaesthesia has been achieved. It has not been possible with existing techniques to examine the changes in BRS that occur during induction of anaesthesia, as measurements of BRS require stationarity for spectral measures, long time segments for sequence methods or a steady state at which interventions such as drug infusions can be performed. Kim & Euler (1997) have introduced an alternative method of estimating BRS from spontaneous heart rate and blood pressure fluctuations based on complex demodulation (CMD) that is capable of assessing the dynamic changes in cardiovascular variability and baroreflex sensitivity as a function of time, and does not assume stationarity of the signal.

In the current study we investigated the changes in baroreflex sensitivity that occur during induction of anaesthesia using CMD in 12 healthy male patients undergoing elective surgery. The injection of propofol 10mg/ml) 0.2ml kg⁻¹, followed by an infusion of 1ml kg⁻¹ hr⁻¹, was associated with a transient tachycardia which commenced on average 25 s after the start of propofol injection. The HR reached a mean peak of 95 bpm at 47 s following the start of the injection of propofol and returned towards pre-anaesthetic rates, plateauing by approximately 84 s. The tachycardia occurred approximately 5 s prior to the onset of hypotension. Approximately 30 s following the start of injection of propofol, systolic and diastolic blood pressure fell, followed by a fall in pulse pressure at 34 s. Systolic pressure fell from a mean of 135 mmHg to 97 mmHg by 60 s after the start of the injection of propofol. BRS decreased to a minima at 35-40 seconds after the start of injection of propofol. On average BRS decreased 38% relative to preinduction levels. Following the initial minima, BRS increased, but in 8 of 12 subjects remained below preanaesthetic levels, while in 4 of 12 subjects BRS was elevated.

We conclude that CMD is a useful tool for examining dynamic changes in BRS, such as those occurring at induction of anaesthesia. The hypotension associated with the initial induction of anaesthesia with propofol cannot be accounted for by the brief initial decrease in BRS but may be caused either by intrathoracic pooling of blood, direct myocardial depression or vasodilatation.

Ebert, T.J., Muzi, M., Berens, R., Goff, D. & Kampine, J.P. (1992) *Anesthesiology*, 76(5):725-33.

Kim S.Y. & Euler D.E. (1997) *Hypertension*, 29, 1119-1125.

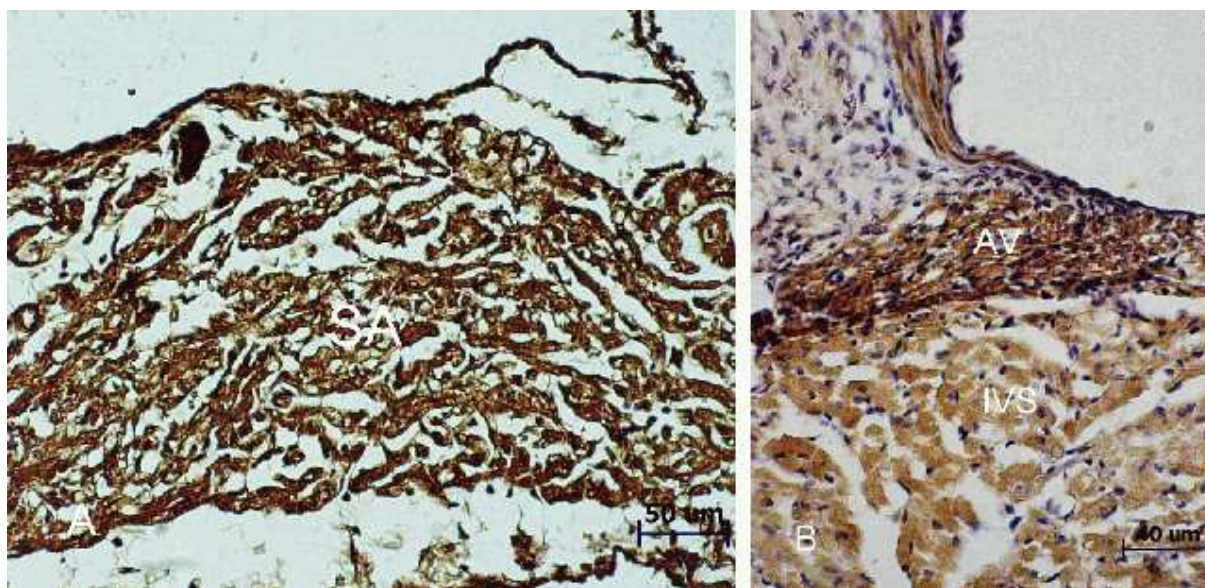
Sellgren, J., Ejnell, H., Elam, M., Ponten, J. & Wallin, B.G. (1994) *Anesthesiology*, 80(3):534-44,.

Calbindin D-28K and parvalbumin calcium-binding proteins in SA and AV nodes of rat heart

S. Vongvatcharanon¹ and U. Vongvatcharanon², ¹Department of Oral and Maxillofacial Surgery (Anesthesiology section), Faculty of Dentistry, and ²Department of Anatomy, Faculty of Science, Prince of Songkla University, Hat-Yai 90112, Thailand.

The role of Ca²⁺-release from the sarcoplasmic reticulum in influencing the pacemaker rate appears to be a common mechanism in sinoatrial node (SA) (Hata *et al.*, 1996) and atrioventricular node (AV) (Hancox *et al.*, 1994). An increased level of intracellular Ca²⁺ or Ca²⁺ overload has been suggested to be a major cause of arrhythmia (Blaustein & Lederer, 1999). Calbindin D-28K and parvalbumin calcium-binding proteins have been found in neurons, and function as intracellular Ca²⁺ buffering transport protein to maintain a constant intracellular Ca²⁺ level (Chard *et al.*, 1993). However, there have been no previous reports of calcium-binding protein in the SA and AV nodes. This study aimed to investigate whether the SA and AV nodes contain calbindin D-28K and parvalbumin.

Adult Wistar rats age 4 weeks were anaesthetised by ether inhalation. The hearts were removed and fixed in 10% formaldehyde. Following dehydration and embedding in paraffin, 5µm serial sections were cut in both the horizontal and coronal planes and then stained with Masson Trichrome to localise the SA and AV nodes. The sections containing SA or AV node were processed for immunohistochemical labeling with antibodies to calbindin D-28K and parvalbumin.



(A) Cross section of the heart at the junction of superior vena cava and right atrium, stained with calbindin D-28K antibody at a dilution of 1:400, showing immunoreactivity (brown color) in the cytoplasm of nodal fibers of SA node. (B) Coronal section of the heart, stained with parvalbumin antibody at a dilution of 1:2000, showing immunoreactivity (brown color) in the cytoplasm of nodal fibers of AV node.

The calbindin D-28K and the parvalbumin are found in both the SA and AV nodes, suggesting these two binding proteins may be involved in the generation and conduction of electrical impulses by maintaining a constant level of the intracellular calcium ions. It is hoped that the study of these calcium binding proteins will open new avenues for therapeutic interventions, especially for the treatment of Ca²⁺ overload and arrhythmia.

Blaustein, M.P. & Lederer, W.J. (1999) *Physiological Review*, 79, 763-854.

Chard, P.S., Bleakman, D., Christakos, S., Fullmer, C.S. & Miller, R.J. (1993) *Journal of Physiology*, 472, 341-357.

Hancox, H., Lederer, W.J. & Cannell, M.B. (1993) *Proceedings of the Royal Society B*, 255, 99-105.

Hata, T., Noda, T., Nishimura, M. & Watanabe, Y. (1996) *Heart and Vessels*, 11, 234-241.

Cardiac remodelling contributes to altered ventricular mechanics in hypertensive cardiomyopathy

A.P. Pope, B.H. Smaill and I.J. LeGrice, Department of Physiology/Bioengineering Institute, University of Auckland, Private Bag 92019 Auckland, New Zealand

The complex organisation of cells and extracellular matrix (ECM) contributes to the diastolic properties of the heart. Remodelling of these structures is a significant feature of cardiovascular diseases such as hypertension and heart failure. The change in the content and organisation of ECM collagen is an important aspect of this remodelling because of the role collagen plays in interconnecting cells and limiting cellular movement during passive filling. The objective of this study was to characterise the differences in 3D collagen organisation in normal and diseased hearts and to link these differences to changes in diastolic function.

Ventricular structure and function measurements were made in Spontaneously Hypertensive rats (SHR) and Wistar-Kyoto (WKY) controls at 12 months. Geometry measurements were made using M-mode echocardiography and systolic blood pressure was measured prior to removal of the hearts. The passive left ventricular (LV) pressure-volume (PV) relationship was characterised for each heart by inflating an LV balloon to a pressure of 30 mmHg. Two hearts from each group were perfused with picosirius red dye via the coronary circulation to stain collagen. Samples from these hearts were resin embedded and imaged using a novel high throughput confocal microscope facility. Imaged blocks were typically 2mm × 0.5mm × 0.3mm with 1µm voxel dimension.

In vivo measurements confirmed that the SHRs were both hypertensive (SHR 152.4mmHg ± 7.7mmHg (n=8), WKY 117.6mmHg±3.8mmHg (n=9), $P=0.001$) and their hearts were hypertrophic (Posterior LV wall thickness: SHR 3.24mm ± 0.24mm (n=6), WKY 2.47mm±0.23mm (n=7), $P=0.042$). Active ventricular function was reduced in the SHR group with fractional shortening at 74.7%± 4.6% (n=6) compared to 61.1%±4.7 % (n=7) in the WKY group ($P=0.07$). The mean LV PV curve for the SHR group was shifted leftward with respect to control. LV stiffness ($\Delta P/\Delta V$) was greater in SHR than in WKY at pressures throughout the range 4 to 28mmHg ($P<0.05$; SHR n=8, WKY n=9).

In WKY blocks, perimysial collagen fibres grouped cells into layers and branched across spaces between the layers whereas the layers in SHR blocks were tightly approximated and there were dense planes of collagen separating them. Furthermore, the epimysial collagen mesh was more obvious in the SHR blocks and both pericellular and perivascular collagen were substantially greater with some regions of cellular necrosis evident.

We believe that these differences in myocardial organisation are responsible for differences in both local and global passive mechanical function. The increased ECM around cells and layers will change cell-to-cell mechanical coupling and limit the ability of myocardial layers to shear relative to each other, likewise increased epimysial collagen will limit ventricular expansion. Additionally, dense collagen around both vessels and individual cells may impair diffusion of oxygen and metabolites and lead to tissue necrosis and scar formation. These changes in local mechanical properties are very likely to be the cause of the reduced ventricular compliance in SHR hearts as compared to WKY and will subsequently result in impaired diastolic function in the diseased hearts.

Autoperfused hindlimb as a physiologically relevant model to study skeletal muscle function and metabolism

A.J. Hoy, G.E. Peoples and P.L. McLennan, Smart Foods Centre, Department of Biomedical Science, University of Wollongong, NSW 2522, Australia.

The aim of this project, was to establish a small animal model that could provide adequate oxygen delivery at physiological vascular resistance to support studies of metabolism and blood flow in both resting and contracting muscle.

Male Hooded Wistar rats were anaesthetised with sodium pentobarbital (6mg/100g body weight i.p.). Polyethylene tubing filled with 0.9% heparinised saline containing 6% w/v dissolved dextran 70 was used as cannulae at all times. The left carotid artery was cannulated to record mean systemic blood pressure. The right femoral artery (non-perfused) was cannulated to supply arterial blood to the left hindlimb femoral artery (perfused) and allow arterial sampling. This loop was passed through a pump for constant flow with perfused hindlimb pressure recorded via a side arm pressure transducer distal to the pump. Passive venous return occurred via a cannula from the left femoral vein to the right external jugular vein, allowing for venous sampling. The left sciatic nerve was stimulated via a bipolar electrode with force produced recorded. Blood was sampled from the venous and arterial loops and oxygen uptake ($\dot{V}O_2$) determined using the Fick equation. Rats were kept normothermic and were ventilated during experiments to control arterial O_2 content. Extracorporeal blood volume was ≤ 2 ml.

At 1 ml·min⁻¹ mean systemic pressure was 99.32 ± 4.06 mmHg (n = 44, mean \pm SEM), mean hindlimb perfusion pressure was 92.31 ± 3.08 mmHg. $\dot{V}O_2$ was 0.328 ± 0.022 $\mu\text{mol}^{-1}\cdot\text{min}^{-1}\cdot\text{gww}^{-1}$ and (a-v) O_2 diff of 5.03 ± 0.35 ml·100ml⁻¹. At 2 ml·min⁻¹ with muscle stimulation mean hindlimb pressure was 166.41 ± 5.16 mmHg (n = 8) with a $\dot{V}O_2$ of 0.570 ± 0.084 $\mu\text{mol}^{-1}\cdot\text{min}^{-1}\cdot\text{gww}^{-1}$ and (a-v) O_2 diff of 4.44 ± 0.69 ml·100ml⁻¹. $\dot{V}O_2$ is decreased at higher flow rates without stimulation (0.190 ± 0.02 $\mu\text{mol}^{-1}\cdot\text{min}^{-1}\cdot\text{gww}^{-1}$) but with muscle contraction was increased. The Table summarises the blood profile during both flow rates.

Arterial		Venous	1ml/min	2ml/min + stim
pH	7.37 ± 0.01	pH	7.27 ± 0.01	7.29 ± 0.01
pCO ₂ (mmHg)	34.77 ± 0.72	pCO ₂ (mmHg)	51.44 ± 1.11	50.60 ± 1.45
pO ₂ (mmHg)	101.47 ± 1.31	pO ₂ (mmHg)	46.33 ± 1.49	45.40 ± 2.52
Hct (%)	45.41 ± 0.42	Hct (%)	47.11 ± 0.42	49.75 ± 0.92
K ⁺ (mmol/l)	3.65 ± 0.04	K ⁺ (mmol/l)	3.33 ± 0.05	3.70 ± 0.05
Hb (g/dL)	14.80 ± 0.14	Hb (g/dL)	15.37 ± 0.14	16.26 ± 0.31
SO ₂ (%)	97.57 ± 0.10	SO ₂ (%)	71.22 ± 1.77	71.69 ± 3.71

The development of an autoperfused rat hindlimb by this laboratory gives rise to a physiologically relevant model to study skeletal muscle function and metabolism.

Vascular remodeling and changes in cellular coupling during vascular disease

N.M. Rummery, S.L. Sandow, T.D. Brackenbury and C.E. Hill, Division of Neuroscience, John Curtin School of Medical Research, Australian National University Canberra, ACT 0200, Australia.

Changes in blood vessel morphology and function, including vascular remodeling and endothelial dysfunction, accompany the increase in peripheral vascular resistance and blood pressure, characteristic of hypertension. Altered gap junction expression has also been described during hypertension (Severs, 1999; Rummery *et al.*, 2002). This study examined the nature of vascular remodeling in two functionally different blood vessels, and correlated this with changes in the distribution of Cxs during the development of hypertension.

The development of hypertension in the spontaneously hypertensive rat (SHR) begins at approximately 4 weeks of age, animals becoming hypertensive compared to age matched control Wistar-Kyoto rats (WKY) at 9 weeks of age (Rummery *et al.*, 2002). In all experiments, rats were anaesthetised with ketamine/rompun (44/8 mg/kg respectively, i.p.) and tissue was prepared for electron microscopy, RNA extraction or immunohistochemistry.

Electron microscopy was used to determine structural characteristics of thoracic aorta (ThA) and caudal artery (CA) obtained from 12 week SHR and WKY. In the CA, but not the ThA, luminal diameter was decreased, while the number of smooth muscle cell layers and the medial cross-sectional area was increased in SHR compared to the WKY. Remodeling of the endothelium was examined in the ThA and CA using immunohistochemistry (IHC). In the 3-week old CA, there was no difference in endothelial cell (EC) morphology between strains, while at 12 weeks, area, length and perimeter of ECs was reduced in SHR. Between 3 and 12 weeks, there was an increase in area and a decrease in length of ECs in WKY, while the area, length and perimeter of ECs in SHR decreased. EC morphology was not different in the ThA of SHR compared to WKY at 12 weeks.

Expression of mRNA and protein for Cxs 37, 40, 43 and 45 was quantified in the ThA and CA of the WKY and SHR using real-time PCR and IHC. At 12 weeks, Cx43 predominated in the ThA, punctate labeling being found in the media. Cx45 was detected in the media of the ThA and CA. Expression of both Cxs was significantly reduced in the SHR. Cx37 was abundantly expressed in the media of the CA, and sparsely in the ThA. This expression did not differ in either artery during hypertension. In the endothelium, Cxs 37, 40, and 43 were detected in both vessels. The density of Cx37 expression was significantly reduced in the endothelium of the ThA in SHR compared to WKY, while Cx40 was decreased in the CA. Between 3 and 12 weeks, the density of Cx40 was reduced in the SHR at 12 weeks compared to 3 weeks of age.

At 3 weeks, mRNA for Cxs 37 and 43 was equally expressed in the ThA of both WKY and SHR, while Cxs 40 and 45 were sparse. In the ThA, expression of protein for Cx43 was similar in both strains, while Cxs 37, 40 and 45 were not detected. In the CA, mRNA for Cx37 was abundantly expressed in both WKY and SHR however expression was significantly less in the WKY. Similarly, mRNA for Cx45 was decreased in the WKY. In the CA, there were no differences in Cx protein expression between strains. Between 3 and 12 weeks, there was no difference in mRNA expression in the ThA. In the CA, mRNA for Cxs 37 and 40 was greater at 3 week compared to 12 weeks in both strains, while Cx45 was greater in the CA of the WKY at 3 weeks. Expression for Cxs 37 and 43 in the ThA was greater in the WKY at 12 compared to 3 weeks. In the CA of both WKY and SHR, protein for Cx45 was greater at 12 compared to 3 weeks, however in the SHR, this was not significant. Expression for Cxs 37, 40 and 43 was not altered in the media of the CA during development.

Results indicate that vascular remodeling occurs in the media and endothelium of muscular but not elastic arteries during hypertension. In the endothelium this remodeling develops coincident with the increasing blood pressure. Changes in Cx expression during hypertension differed depending on the vessel studied, with significant changes occurring with the development of hypertension. The changes described here may have significant consequences for blood vessel function during the development of hypertension.

Severs, N.J. (1999) *Novartis Foundation Symposium*, 219:188-211.

Rummery, N.M., McKenzie, K.U.S., Whitworth, J.A. & Hill, C.E. (2002) *Journal of Hypertension*, 20:247-253.

Initiation and coordination of vasomotion in rat cerebral arteries

R.E. Haddock, T.D. Brackenbury and C.E. Hill, Division of Neuroscience, John Curtin School of Medical Research, Australian National University, Canberra, ACT 2601, Australia.

In cerebral blood vessels, rhythmical contractions in vessel diameter, or vasomotion, play an important role in determining blood flow and vascular resistance. In mesenteric arteries, the endothelium and cGMP have been shown to be essential for initiating vasomotion, presumably through the release of nitric oxide (NO) (Peng *et al.*, 2001), while cell coupling is suggested to coordinate calcium oscillations (Sell *et al.*, 2002). Vasomotion in the basilar artery is dependent on intracellular calcium stores and an interplay between voltage activated calcium and potassium channels (Haddock & Hill, 2002), while the role of the endothelium and cell coupling is unknown. We have therefore investigated the role and distribution of vascular connexins (Cx) and the role of the endothelium in the initiation and coordination of vasomotion in the juvenile rat basilar artery.

Wistar rats (14-17 days) were anaesthetised with ether and decapitated (Animal Experimentation Ethics Committee, ANU). The basilar artery and its branches were isolated and pinned in a recording chamber which was perfused with physiological saline. Changes in membrane potential were measured with sharp microelectrodes (140-220 M Ω), which were filled with propidium iodide to identify the impaled cells. Changes in arterial wall or individual smooth muscle cell (SMC) intracellular calcium ($[Ca^{2+}]_i$) were assessed using Fura 2-AM, and either photometry or an intensified CCD camera respectively. Contractions of the same vessels were simultaneously recorded using videomicroscopy. Immunohistochemistry was performed on intact vessels following perfusion fixation (2% paraformaldehyde in phosphate buffer) and imaged using confocal microscopy. Serial section electron microscopy was used to investigate the presence of myoendothelial gap junctions (MEJGs).

Under control conditions, rhythmical depolarisations and $[Ca^{2+}]_i$ oscillations in both the arterial wall and in individual SMCs preceded rhythmical contractions. Membrane potential recordings from either SMCs or ECs were not significantly different and serial section electron microscopy confirmed that MEJGs connected the endothelium to the SMCs. The NOS inhibitor L-NAME (10 μ M) and the selective guanylate cyclase inhibitor ODQ (10 μ M) increased the frequency and amplitude of rhythmical activity and constricted the vessel. ODQ, but not L-NAME, hyperpolarised the vessel. Removal of the endothelium resulted in irregular contractions, asynchronous $[Ca^{2+}]_i$ oscillations in adjacent SMCs and a small depolarisation of the vessel. Addition of ODQ to endothelial denuded preparations prevented the constriction and augmentation of residual rhythmical activity induced by cGMP inhibition, but had no effect on the hyperpolarisation. Cx37, 40 and 43, but not Cx45, were found in the endothelium, while Cx 37, 43 and 45 were expressed to a lesser extent in SMCs. The gap junction uncoupler ^{37,43}Gap 27 (100 μ M) abolished rhythmical activity and hyperpolarised the SMCs, while ⁴⁰Gap 27 resulted in irregular contractions and asynchronous $[Ca^{2+}]_i$ oscillations in SMCs, but had no effect on membrane potential.

We conclude that the endothelium is essential for the coordination but not initiation of $[Ca^{2+}]_i$ oscillations and vasomotion in the basilar artery. This does not occur through the release of NO and activation of a depolarising current, but may instead be due to electrical coupling through MEJGs containing Cx40. The hyperpolarisation caused by ODQ suggests effects on ion channels of additional cGMP within SMCs. The persistence of vasomotion in the presence of ODQ confirms that cGMP was also not responsible for the initiation of vasomotion. Together the data indicate that the mechanism responsible for the initiation of vasomotion in cerebral arteries differs from that in systemic vessels.

Haddock R.E. & Hill C.E. (2002) *Journal of Physiology*, 545, 615-627.

Peng H., Matchkov V., Ivarsen A., Aalkjaer C. & Nilsson H. (2001) *Circulation Research*, 88, 810-815.

Sell M., Boldt W. & Markwardt F. (2002) *Cell Calcium*, 3, 105-120.

Functional remodeling in response to prolonged agonist exposure or elevated pressure delays arteriolar relaxation

S.J. Potocnik¹, M.A. Hill¹, L.A. Martinez-Lemus² and G.A. Meininger², ¹Microvascular Biology Group, School of Medical Sciences, RMIT University, Melbourne, Vic. 3081 Australia and

²Department of Medical Physiology, College of Medicine, Texas A&M University, College Station, Texas 77843, USA.

While arteriolar contraction is dependent on Ca²⁺- induced myosin phosphorylation, other mechanisms including Ca²⁺ sensitisation and time-dependent phenomena such as cytoskeletal and cellular reorganisation may contribute to contractile events. We have hypothesised that if arteriolar smooth muscle exhibits time-dependent behavior that this may be manifested in differences in relaxation following short and long-term exposure to contractile agonists. Consistent with this, isolated skeletal muscle arterioles showed a significantly delayed return to pre-agonist exposure diameter following washout of noradrenaline (5µM) which had been applied for 4 hours as compared to 5 minutes. A similar phenomenon was not observed when contraction was induced by KCl (75 mM) suggesting a possible requirement for receptor activation. As removal of extracellular Ca²⁺ caused a rapid return to passive diameter, the delayed relaxation following 4 h norepinephrine exposure was viewed as being functional in character. The enhanced constrictor response following prolonged norepinephrine exposure was prevented by several tyrosine kinase inhibitors (genistein, PP1 and PD9859; Hill *et al.*, 2003). Arterioles were cannulated onto glass micropipettes and studied *in vitro* using video microscopy, following dissection (4°C) from the cremaster muscle, sampled from anaesthetised rats. Further studies presented here showed that the impaired relaxation is not inhibited in the presence of the Rho kinase inhibitor Y27632. This observation suggests the mechanism is not due to Rho kinase-induced Ca²⁺ sensitisation events contributing to an enhanced constrictor response, while the former implicates events involving a cSrc/p42/44 MAP kinase pathway. In these spontaneously myogenic arterioles, the constrictor stimulus of elevated intraluminal pressure, from 50 to 120 mmHg for 4 hours also results in delayed myogenic vasodilation when the luminal pressure is returned to 50 mmHg. Confocal microscopy studies (using a fluorescein dye exclusion imaging method) aimed at examining smooth muscle cell position within the intact vessel wall suggested that cellular realignment occurs during the 4 hour agonist exposure, consistent with the proposition that early remodelling events are occurring during this 4 hour time course. In particular, an increase in the extent of overlap between neighbouring vascular smooth muscle cells was observed after the prolonged agonist exposure period. Collectively, these data are consistent with the action of prolonged constrictor stimuli, either noradrenaline exposure or elevated luminal pressure, resulting in an early functional remodelling process that involves tyrosine kinase-dependent processes and results in impaired relaxation on removal of the stimulus.

Hill, M.A., Potocnik, S.J., Martinez, L.A. & Meininger, G.A. (2003) *American Journal of Physiology*, 285:H849-H856.